

# High-pressure Syntheses, Crystal Structures, and Thermal Behaviour of $\beta$ - $RE(\text{BO}_2)_3$ ( $RE = \text{Nd}, \text{Sm}, \text{Gd}$ )

Holger Emme, Gunter Heymann, Almut Haberer, and Hubert Huppertz

Department Chemie und Biochemie, Ludwig-Maximilians-Universität München,  
Butenandtstraße 5–13 (Haus D), 81377 München, Germany

Reprint requests to H. Huppertz. E-mail: huh@cup.uni-muenchen.de

*Z. Naturforsch.* **2007**, 62b, 765–770; received February 6, 2007

The compounds  $\beta$ - $RE(\text{BO}_2)_3$  [ $RE = \text{Nd}$  (neodymium *meta*-borate),  $\text{Sm}$  (samarium *meta*-borate) and  $\text{Gd}$  (gadolinium *meta*-borate)] were synthesized under high-pressure and high-temperature conditions in a Walker-type multianvil apparatus at 3.5 GPa ( $\text{Nd}$ ), 7.5 GPa ( $\text{Sm}$ ,  $\text{Gd}$ ) and 1050 °C. The crystal structures were determined by single crystal X-ray diffraction data collected at r. t. ( $\text{Sm}$ ,  $\text{Gd}$ ) and at  $-73$  °C ( $\text{Nd}$ ), respectively. The structures are isotypic with the already known ambient-pressure phases  $\beta$ - $RE(\text{BO}_2)_3$  ( $RE = (\text{Tb}, \text{Dy})$ ) and the high-pressure phases  $\beta$ - $RE(\text{BO}_2)_3$  ( $RE = \text{Ho–Lu}$ ).

**Key words:** High-pressure Phases, Borates, Crystal Structure

## Introduction

In recent years, a systematic investigation of rare earth *meta*-borates with the composition  $RE(\text{BO}_2)_3$  under ambient- and high-pressure conditions led to the discovery of new modifications and the clarification of the stability ranges. Up to now, four modifications of rare earth *meta*-borates are known, designated chronologically as  $\alpha$ -,  $\beta$ -,  $\gamma$ -, and  $\delta$ - $RE(\text{BO}_2)_3$ . The monoclinic phases  $\alpha$ - $RE(\text{BO}_2)_3$  ( $RE = \text{La}$  [1, 2],  $\text{Ce}$  [3],  $\text{Pr}$  [4],  $\text{Nd}$  [5, 6],  $\text{Sm}$  [7],  $\text{Eu}$  [8],  $\text{Gd}$  [7],  $\text{Tb}$  [9]) crystallize in the space group  $I2/a$ . They are built up of chains of triangular  $[\text{BO}_3]^{3-}$  and tetrahedral  $[\text{BO}_4]^{5-}$  units, representing the longest known phases. In 2003, Nikelski and Schleid solved the structure of the second polymorph  $\beta$ - $RE(\text{BO}_2)_3$  ( $RE = \text{Tb}$ ), built up exclusively of  $[\text{BO}_4]^{5-}$  tetrahedra, forming corrugated layers [10]. This second modification was also observed with  $RE = \text{Dy}$  under ambient-pressure conditions. However, the synthesis of the  $\beta$ -modification with the smaller rare earth cations  $\text{Ho–Lu}$  required the use of high-pressure / high-temperature conditions (7.5 GPa, 1273 K) [11]. In 2004, we were able to realize a third modification  $\gamma$ - $RE(\text{BO}_2)_3$  with the larger rare earth cations  $\text{La–Nd}$  at 7.5 GPa and 1273 K, which exhibits a highly condensed network of  $[\text{BO}_4]^{5-}$  tetrahedra [12]. Due to the remarkable difference between ambient-pressure conditions and 7.5 GPa, we investigated the pressure range below 7.5 GPa and discovered a fourth modification,  $\delta$ - $RE(\text{BO}_2)_3$ , at 5.5 GPa

and 1323 K with the rare earth cations  $\text{La}^{3+}$  and  $\text{Ce}^{3+}$  [13, 14]. In accordance with the pressure coordination rule,  $\delta$ - $RE(\text{BO}_2)_3$  consists exclusively of  $[\text{BO}_4]^{5-}$  tetrahedra in contrast to the  $\alpha$ -modification, which exhibits  $[\text{BO}_3]^{3-}$  and  $[\text{BO}_4]^{5-}$  units. In principle, compounds exhibiting  $[\text{BO}_3]^{3-}$  groups can be transformed into more dense modifications with  $[\text{BO}_4]^{5-}$  groups. Therefore, we tried to synthesize more dense modifications of  $\alpha$ - $RE(\text{BO}_2)_3$  ( $RE = \text{Nd}, \text{Sm}, \text{Gd}$ ) under high pressure. We succeeded in the transformation into the phases  $\beta$ - $RE(\text{BO}_2)_3$  ( $RE = \text{Nd}, \text{Sm}$ , and  $\text{Gd}$ ), about which we report below.

## Experimental Section

The starting materials for the syntheses of  $\beta$ - $RE(\text{BO}_2)_3$  ( $RE = \text{Nd}, \text{Sm}, \text{Gd}$ ) were 3 : 1 molar mixtures of  $\text{B}_2\text{O}_3$  (Strem Chemicals, Newburyport, USA; 99.9 %) with the rare earth oxides  $RE_2\text{O}_3$  ( $RE = \text{Nd}, \text{Sm}, \text{Gd}$ ; 99.9 %). The compounds were compressed and heated *via* a multianvil assembly. Details of the assembly can be found in the literature [15–18]. For the synthesis of  $\beta$ - $\text{Nd}(\text{BO}_2)_3$ , an 18/11 assembly was compressed within 80 min to 3.5 GPa and heated to 1323 K in the following 25 min. Having maintained this temperature for 5 min, the sample was cooled to about 700 K during further 25 min. Afterwards, the sample was quenched to r. t. For the syntheses of  $\beta$ - $RE(\text{BO}_2)_3$  ( $RE = \text{Sm}, \text{Gd}$ ), an 18/11 ( $\text{Gd}$ ) and an 14/8 assembly ( $\text{Sm}$ ) were compressed within 3 h (18/11) / 2 h (14/8) up to 7.5 GPa and heated up to 1323 K in the following 10 min. Having kept this temperature for 10 min, the samples were cooled down to r. t. within 10 min. After the de-

Empirical formula	$\beta$ -Nd(BO <sub>2</sub> ) <sub>3</sub>	$\beta$ -Sm(BO <sub>2</sub> ) <sub>3</sub>	$\beta$ -Gd(BO <sub>2</sub> ) <sub>3</sub>
Molar mass [g mol <sup>-1</sup> ]	272.67	278.78	285.68
Unit cell dimensions			
<i>a</i> [pm]	1616.2(3)	1612.5(2)	1602.8(2)
<i>b</i> [pm]	747.4(2)	746.02(4)	742.70(4)
<i>c</i> [pm]	1244.2(3)	1240.87(7)	1232.17(7)
<i>V</i> [nm <sup>3</sup> ]	1.5028(5)	1.4927(2)	1.4668(2)
Calculated density [g cm <sup>-3</sup> ]	4.82	4.96	5.18
Crystal size [ $\mu$ m <sup>3</sup> ]	50 × 35 × 30	60 × 40 × 20	60 × 50 × 50
Temperature [°C]	−73(2)	20(2)	20(2)
Detector distance [mm]	40	40	45
Exposure time [min]	14	10	15
$\omega$ range [°]; increment [°]	0–180; 1.2	0–180; 1.1	0–180; 1.2
Transm. ratio [max/min]	0.469 / 0.663	0.319 / 0.595	0.414 / 0.487
Absorption coefficient [mm <sup>-1</sup> ]	13.8	15.7	18.0
<i>F</i> (000)	1968	2000	2032
$\theta$ range [°]	3.2 to 31.0	3.4 to 30.0	3.0 to 31.6
Range in <i>hkl</i>	±23, ±10, ±18	±22, ±9, −17/+15	±23, ±10, −18/+17
Total no. reflections	16464	15072	16539
Independent reflections	2550 ( <i>R</i> <sub>int</sub> = 0.080)	2209 ( <i>R</i> <sub>int</sub> = 0.149)	2490 ( <i>R</i> <sub>int</sub> = 0.066)
Reflections with <i>I</i> ≥ 2σ( <i>I</i> )	1897 ( <i>R</i> <sub>σ</sub> = 0.060)	1587 ( <i>R</i> <sub>σ</sub> = 0.089)	1813 ( <i>R</i> <sub>σ</sub> = 0.066)
Data/parameters	2550 / 167	2209 / 169	2490 / 196
Goodness-of-fit on <i>F</i> <sup>2</sup>	0.927	0.855	0.796
Final <i>R</i> indices [ <i>I</i> ≥ 2σ( <i>I</i> )]	<i>R</i> 1 = 0.042 <i>wR</i> 2 = 0.097	<i>R</i> 1 = 0.034 <i>wR</i> 2 = 0.066	<i>R</i> 1 = 0.020 <i>wR</i> 2 = 0.031
<i>R</i> indices (all data)	<i>R</i> 1 = 0.063 <i>wR</i> 2 = 0.102	<i>R</i> 1 = 0.056 <i>wR</i> 2 = 0.070	<i>R</i> 1 = 0.041 <i>wR</i> 2 = 0.033
Largest diff. peak / hole [e Å <sup>-3</sup> ]	2.86 / −2.93	2.09 / −2.22	1.12 / −1.31

Table 1. Crystal data and structure refinement for  $\beta$ -RE(BO<sub>2</sub>)<sub>3</sub> (RE = Nd, Sm, Gd), space group *Pnma*, *Z* = 16.

compression of the assemblies the recovered octahedral pressure media were broken apart. The samples were carefully separated from the surrounding boron nitride crucibles. The compounds  $\beta$ -RE(BO<sub>2</sub>)<sub>3</sub> (RE = Nd, Sm, Gd) were gained as single-phase crystalline products [yield: *ca.* 75 mg (18/11) / *ca.* 40 mg (14/8) per run]. The substances are air- and water-resistant, crystallizing as thin colourless (Sm, Gd) and pale-pink (Nd) platelets.

#### Crystal structure analysis

Small, irregularly shaped single crystals of the compounds  $\beta$ -RE(BO<sub>2</sub>)<sub>3</sub> (RE = Nd, Sm, Gd) were first examined through a Buerger camera, equipped with an image plate system (Fujifilm BAS-1800) in order to establish both the symmetry and the suitability for intensity data collection. The single crystal intensity data were collected at r. t. (Sm, Gd) and at −73 °C (Nd) by a Stoe IPDS-I diffractometer with graphite-monochromatized MoK $\alpha$  radiation ( $\lambda$  = 71.073 pm). For  $\beta$ -Nd(BO<sub>2</sub>)<sub>3</sub>, an empirical absorption correction was applied on the basis of  $\psi$ -scan data. A numerical absorption correction (HABITUS [19]) was used for the data of  $\beta$ -RE(BO<sub>2</sub>)<sub>3</sub> (RE = Sm and Gd). All relevant details of the data collections and evaluations are listed in Table 1. The atomic parameters of  $\beta$ -Dy(BO<sub>2</sub>)<sub>3</sub> [11] were taken as starting values for all three *meta*-borates, and the structures were refined by full-matrix least-squares on *F*<sup>2</sup> using SHELXL-97 [20]. Anisotropic atomic displacement param-

Table 2. Atomic coordinates and isotropic equivalent displacement parameters *U*<sub>eq</sub> (Å<sup>2</sup>) for  $\beta$ -Nd(BO<sub>2</sub>)<sub>3</sub> (space group *Pnma*). *U*<sub>eq</sub> is defined as one third of the trace of the orthogonalized *U*<sub>ij</sub> tensor.

Atom	Wyckoff-Position	<i>x</i>	<i>y</i>	<i>z</i>	<i>U</i> <sub>eq</sub>
Nd1	4 <i>c</i>	0.17059(4)	1/4	0.92991(5)	0.0061(2)
Nd2	4 <i>c</i>	0.12034(4)	3/4	0.00416(5)	0.0071(2)
Nd3	4 <i>c</i>	0.04745(4)	1/4	0.58560(5)	0.0064(2)
Nd4	4 <i>c</i>	0.12564(4)	3/4	0.72233(5)	0.0070(2)
B1	8 <i>d</i>	0.2831(6)	0.931(2)	0.8123(7)	0.008(2)
B2	8 <i>d</i>	0.9403(5)	0.928(2)	0.6558(7)	0.005(2)
B3	8 <i>d</i>	0.0273(6)	0.061(2)	0.8199(8)	0.008(2)
B4	8 <i>d</i>	0.1554(5)	0.928(2)	0.4817(7)	0.005(2)
B5	8 <i>d</i>	0.1105(5)	0.079(2)	0.1458(7)	0.007(2)
B6	8 <i>d</i>	0.2568(5)	0.932(2)	0.1297(7)	0.005(2)
O1	4 <i>c</i>	0.1616(6)	3/4	0.5321(7)	0.009(2)
O2	8 <i>d</i>	0.2816(4)	0.0558(8)	0.8997(5)	0.006(2)
O3	8 <i>d</i>	0.9270(4)	0.0496(8)	0.5665(5)	0.008(2)
O4	8 <i>d</i>	0.0500(4)	0.9386(7)	0.1254(5)	0.005(2)
O5	8 <i>d</i>	0.3701(4)	0.9274(7)	0.7665(5)	0.007(2)
O6	8 <i>d</i>	0.1852(3)	0.0352(7)	0.0813(4)	0.005(2)
O7	4 <i>c</i>	0.0596(5)	1/4	0.8012(7)	0.007(2)
O8	4 <i>c</i>	0.2256(5)	3/4	0.1363(7)	0.009(2)
O9	8 <i>d</i>	0.0930(4)	0.9636(7)	0.8723(5)	0.007(2)
O10	8 <i>d</i>	0.1666(4)	0.0584(8)	0.5675(5)	0.007(2)
O11	4 <i>c</i>	0.0796(5)	1/4	0.1105(6)	0.004(2)
O12	4 <i>c</i>	0.2556(5)	3/4	0.8503(7)	0.006(2)
O13	4 <i>c</i>	0.0471(6)	1/4	0.3911(8)	0.009(2)
O14	8 <i>d</i>	0.0171(4)	0.9846(8)	0.7087(5)	0.007(2)
O15	8 <i>d</i>	0.2249(4)	0.9861(9)	0.7323(5)	0.008(2)

Table 3. Atomic coordinates and isotropic equivalent displacement parameters  $U_{eq}$  (Å<sup>2</sup>) for  $\beta$ -Sm(BO<sub>2</sub>)<sub>3</sub> (space group  $Pnma$ ).  $U_{eq}$  is defined as one third of the trace of the orthogonalized  $U_{ij}$  tensor.

Atom	Wyckoff-Position	x	y	z	$U_{eq}$
Sm1	4c	0.17139(3)	1/4	0.93085(4)	0.0087(2)
Sm2	4c	0.12001(3)	3/4	0.00528(5)	0.0115(2)
Sm3	4c	0.04787(3)	1/4	0.58599(4)	0.0088(2)
Sm4	4c	0.12643(3)	3/4	0.72539(4)	0.0096(2)
B1	8d	0.2831(6)	0.929(2)	0.8130(7)	0.011(2)
B2	8d	0.9416(5)	0.929(2)	0.6557(7)	0.009(2)
B3	8d	0.0296(5)	0.060(2)	0.8207(7)	0.010(2)
B4	8d	0.1551(5)	0.921(2)	0.4808(7)	0.008(2)
B5	8d	0.1101(5)	0.078(2)	0.1445(7)	0.009(2)
B6	8d	0.2562(5)	0.932(2)	0.1288(7)	0.007(2)
O1	4c	0.1605(4)	3/4	0.5340(6)	0.007(2)
O2	8d	0.2821(3)	0.0590(8)	0.8989(4)	0.010(2)
O3	8d	0.9276(3)	0.0519(9)	0.5671(4)	0.010(2)
O4	8d	0.0491(3)	0.9363(8)	0.1239(4)	0.011(2)
O5	8d	0.3706(3)	0.9272(7)	0.7656(4)	0.008(2)
O6	8d	0.1849(3)	0.0341(8)	0.0801(4)	0.009(2)
O7	4c	0.0609(4)	1/4	0.8020(6)	0.009(2)
O8	4c	0.2246(4)	3/4	0.1383(6)	0.009(2)
O9	8d	0.0940(3)	0.9617(8)	0.8742(4)	0.010(2)
O10	8d	0.1665(3)	0.0600(8)	0.5662(4)	0.009(2)
O11	4c	0.0776(5)	1/4	0.1082(6)	0.010(2)
O12	4c	0.2562(5)	3/4	0.8528(6)	0.010(2)
O13	4c	0.0473(5)	1/4	0.3922(6)	0.010(2)
O14	8d	0.0189(3)	0.9834(8)	0.7078(4)	0.010(2)
O15	8d	0.2247(3)	0.9839(9)	0.7303(5)	0.011(2)

Table 4. Atomic coordinates and isotropic equivalent displacement parameters  $U_{eq}$  (Å<sup>2</sup>) for  $\beta$ -Gd(BO<sub>2</sub>)<sub>3</sub> (space group  $Pnma$ ).  $U_{eq}$  is defined as one third of the trace of the orthogonalized  $U_{ij}$  tensor.

Atom	Wyckoff-Position	x	y	z	$U_{eq}$
Gd1	4c	0.17134(2)	1/4	0.93258(2)	0.00408(7)
Gd2	4c	0.12070(2)	3/4	0.00677(2)	0.00421(7)
Gd3	4c	0.04789(2)	1/4	0.58769(2)	0.00432(7)
Gd4	4c	0.12680(2)	3/4	0.72781(2)	0.00431(7)
B1	8d	0.2825(3)	0.9301(8)	0.8136(4)	0.005(2)
B2	8d	0.9416(3)	0.9267(8)	0.6540(4)	0.004(2)
B3	8d	0.0311(3)	0.0608(8)	0.8217(4)	0.006(2)
B4	8d	0.1541(3)	0.9235(7)	0.4831(4)	0.006(2)
B5	8d	0.1100(3)	0.0767(7)	0.1439(4)	0.0045(9)
B6	8d	0.2575(3)	0.9304(8)	0.1297(4)	0.0045(9)
O1	4c	0.1607(2)	3/4	0.5376(3)	0.0037(9)
O2	8d	0.2819(2)	0.0622(5)	0.8992(5)	0.0047(7)
O3	8d	0.9292(2)	0.0537(5)	0.5663(2)	0.0035(6)
O4	8d	0.0492(2)	0.9358(4)	0.1238(2)	0.0041(6)
O5	8d	0.3705(2)	0.9259(4)	0.7655(2)	0.0029(6)
O6	8d	0.1853(2)	0.0350(5)	0.0789(2)	0.0036(6)
O7	4c	0.0627(3)	1/4	0.8015(3)	0.0061(9)
O8	4c	0.2249(2)	3/4	0.1391(3)	0.0038(9)
O9	8d	0.0948(2)	0.9605(5)	0.8756(2)	0.0050(6)
O10	8d	0.1655(2)	0.0625(4)	0.5661(2)	0.0037(6)
O11	4c	0.0791(2)	1/4	0.1079(3)	0.0038(9)
O12	4c	0.2553(3)	3/4	0.8535(3)	0.0060(9)
O13	4c	0.0484(3)	1/4	0.3952(3)	0.0048(9)
O14	8d	0.0197(2)	0.9793(5)	0.7088(2)	0.0039(7)
O15	8d	0.2240(2)	0.9828(5)	0.7314(2)	0.0048(7)

ters were used for all atoms except the boron atoms of  $\beta$ -Nd(BO<sub>2</sub>)<sub>3</sub>, which were refined isotropically. The final difference Fourier syntheses revealed no significant residual peaks in all refinements. The positional parameters are listed in Tables 2–4. Anisotropic displacement parameters, interatomic distances, and interatomic angles are available from the Fachinformationszentrum Karlsruhe, D-76344 Eggenstein-Leopoldshafen (Germany), by quoting the Registry No's. CSD-417645 ( $\beta$ -Nd(BO<sub>2</sub>)<sub>3</sub>), CSD-417643 ( $\beta$ -Sm(BO<sub>2</sub>)<sub>3</sub>), and CSD-417644 ( $\beta$ -Gd(BO<sub>2</sub>)<sub>3</sub>).

## Results and Discussion

Fig. 1 shows a view of the crystal structure of  $\beta$ -RE(BO<sub>2</sub>)<sub>3</sub>, which is composed of strongly corrugated layers of corner sharing [BO<sub>4</sub>]<sup>5-</sup> tetrahedra. A detailed description of this structure type can be found in the references [10] and [11]. The characteristic aspects of the new compounds are briefly reported in the following.

The B–O bond lengths in  $\beta$ -RE(BO<sub>2</sub>)<sub>3</sub> (RE = Nd, Sm, Gd) are in the range of 142.3(2)–153.4(2) pm in  $\beta$ -Nd(BO<sub>2</sub>)<sub>3</sub>, 143.3(2)–153.5(2) pm in  $\beta$ -Sm(BO<sub>2</sub>)<sub>3</sub>, and 142.8(6)–153.1(5) pm in  $\beta$ -Gd(BO<sub>2</sub>)<sub>3</sub>, similar to

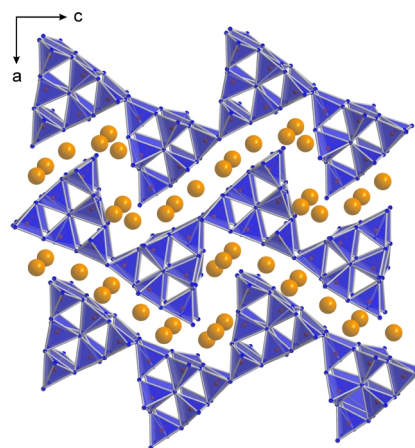


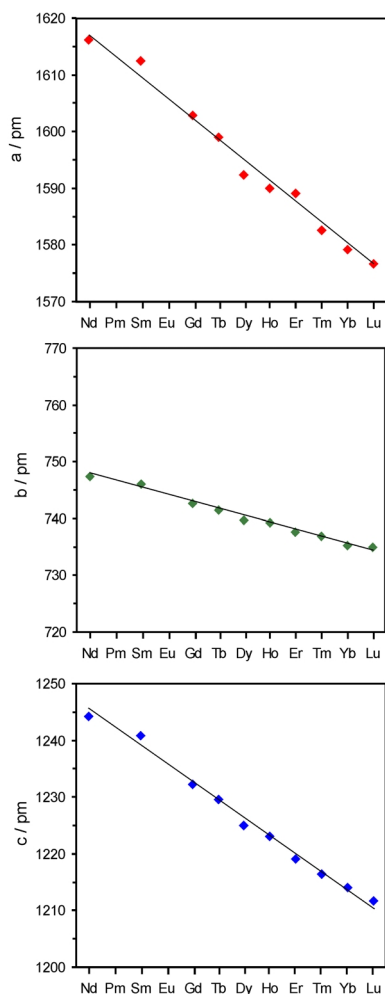
Fig. 1. Crystal structure of the *meta*-borates  $\beta$ -RE(BO<sub>2</sub>)<sub>3</sub> (RE = Nd, Sm, Gd).

the B–O bond lengths found in the isotypic compounds with RE = Tb–Lu. The distances Nd–O, Sm–O, and Ho–O are in the ranges 233.1(6)–296.0(6), 230.6(6)–289.9(7), and 228.6(3)–286.7(4) pm, respectively. The B–O bond lengths of the three-coordinate O(5) atoms in the [OB<sub>3</sub>]<sup>7+</sup> groups of the compounds vary in the

Table 5. Comparison of the lattice parameters (pm) and volumes (nm<sup>3</sup>) of RE(BO<sub>2</sub>)<sub>3</sub> (RE = Tb–Lu).

Compound	<i>a</i>	<i>b</i>	<i>c</i>	<i>V</i>
$\beta$ -Nd(BO <sub>2</sub> ) <sub>3</sub> [*]	1616.2(3)	747.4(2)	1244.2(3)	1.503(1)
$\beta$ -Sm(BO <sub>2</sub> ) <sub>3</sub> [*]	1612.5(2)	746.02(4)	1240.87(7)	1.492(1)
$\beta$ -Gd(BO <sub>2</sub> ) <sub>3</sub> [*]	1602.9(2)	742.70(4)	1232.17(7)	1.467(1)
$\beta$ -Tb(BO <sub>2</sub> ) <sub>3</sub> [10]	1598.97(9)	741.39(4)	1229.58(7)	1.458(1)
$\beta$ -Dy(BO <sub>2</sub> ) <sub>3</sub> [11]	1592.4(1)	739.7(1)	1225.0(1)	1.443(1)
$\beta$ -Ho(BO <sub>2</sub> ) <sub>3</sub> [11]	1590.0(4)	739.3(2)	1223.1(4)	1.438(1)
$\beta$ -Er(BO <sub>2</sub> ) <sub>3</sub> [11]	1589.1(2)	737.6(1)	1219.1(1)	1.429(1)
$\beta$ -Tm(BO <sub>2</sub> ) <sub>3</sub> [11]	1582.6(3)	736.8(3)	1216.4(3)	1.418(1)
$\beta$ -Yb(BO <sub>2</sub> ) <sub>3</sub> [11]	1579.1(3)	735.2(2)	1214.0(3)	1.410(1)
$\beta$ -Lu(BO <sub>2</sub> ) <sub>3</sub> [11]	1576.7(3)	734.9(2)	1211.7(3)	1.404(1)

\* This work.

Fig. 2. Plot of the lattice parameters of the rare earth *meta*-borates  $\beta$ -RE(BO<sub>2</sub>)<sub>3</sub> (RE = Nd–Lu, except Pm and Eu).

ranges 149.1(2)–153.4(2) pm in Nd(BO<sub>2</sub>)<sub>3</sub>, 150.4(2)–153.5(2) pm in Sm(BO<sub>2</sub>)<sub>3</sub>, and 151.0(2)–153.1(5) pm in Gd(BO<sub>2</sub>)<sub>3</sub>.

Table 5 and Fig. 2 present a survey of the lattice parameters of all known  $\beta$ -RE(BO<sub>2</sub>)<sub>3</sub> phases (RE = Nd–Lu except Pm and Eu). The new *meta*-borates fit well into the scheme of the known compounds. Nd<sup>3+</sup>, Sm<sup>3+</sup>, and Gd<sup>3+</sup> represent the largest rare earth ions in this series, and here we also observe the trend towards a much more slowly decreasing lattice parameter *b* in contrast to *a* and *c*, as we already noted for the compounds  $\beta$ -RE(BO<sub>2</sub>)<sub>3</sub> (RE = Dy–Lu). This is caused by the ability to contract more strongly along the *a* and *c* direction in the crystal structure (Fig. 1), in contrast to *b* (layers of [BO<sub>4</sub>]<sup>5−</sup> tetrahedra), in accordance with the shrinking radius of the RE<sup>3+</sup> ions (lanthanoid contraction).

Fig. 3 illustrates the modifications of all rare earth *meta*-borates synthesized up to now. The scheme distinguishes between syntheses under ambient- (X) and high-pressure (Ø) conditions. Next to La(BO<sub>2</sub>)<sub>3</sub>, which can be synthesized in three different modifications ( $\alpha$ ,  $\beta$ ,  $\delta$ ), Nd(BO<sub>2</sub>)<sub>3</sub> is the second example, that can be synthesized in three different structures ( $\alpha$ ,  $\beta$ ,  $\gamma$ ), depending on the applied pressure. Up to now, it is not clear if the phases  $\beta$ -RE(BO<sub>2</sub>)<sub>3</sub> (RE = Nd, Sm, Gd) can also be synthesized under ambient-pressure conditions, as it is possible for RE = Tb, Dy. However, high-pressure conditions favour the formation of the  $\beta$ -modifications due to the densification effect [21]. At pressures of 3.5 GPa (Nd) and 7.5 GPa (Sm, Gd) the compounds crystallize in the orthorhombic  $\beta$ -RE(BO<sub>2</sub>)<sub>3</sub> structure, possessing a higher density than the corresponding  $\alpha$ -phases. *E. g.*,  $\alpha$ -Nd(BO<sub>2</sub>)<sub>3</sub> has a density of 4.50 g cm<sup>−3</sup> and the more dense modification  $\beta$ -Nd(BO<sub>2</sub>)<sub>3</sub> presented here exhibits a value of 4.82 g cm<sup>−3</sup>. In analogy,  $\beta$ -Sm(BO<sub>2</sub>)<sub>3</sub> and  $\beta$ -Gd(BO<sub>2</sub>)<sub>3</sub> possess values of 4.96 and 5.18 g cm<sup>−3</sup>, which are higher than the densities of the  $\alpha$ -modifications with 4.63 and 4.84 g cm<sup>−3</sup>, respectively.

#### Thermal behaviour of $\beta$ -Sm(BO<sub>2</sub>)<sub>3</sub> and $\beta$ -Gd(BO<sub>2</sub>)<sub>3</sub>

*In situ* X-ray powder diffraction experiments were performed on a STOE STADI P powder diffractometer (MoK $\alpha$  radiation,  $\lambda$  = 71.073 pm) with a computer controlled STOE furnace: The sample was enclosed in a quartz capillary and heated from r. t. to 500 °C in 100 °C steps, and from 500 °C to 1100 °C in 50 °C steps. Afterwards, the sample was cooled down to 500 °C in 50 °C steps, and from 500 °C to r. t. in

	La	Ce	Pr	Nd	Pm	Sm	Eu	Gd	Tb	Dy	Ho	Er	Tm	Yb	Lu
$\alpha$ - $RE(\text{BO}_2)_3$	X	X	X	X		X	X	X	X						
$\beta$ - $RE(\text{BO}_2)_3$				Ø		Ø		Ø	X	X	Ø	Ø	Ø	Ø	Ø
$\gamma$ - $RE(\text{BO}_2)_3$	Ø	Ø	Ø	Ø											
$\delta$ - $RE(\text{BO}_2)_3$	Ø														

X Ambient-pressure conditions; Ø High-pressure conditions.

Fig. 3. Schematic view of the existing modifications of the rare earth *meta*-borates  $RE(\text{BO}_2)_3$ .

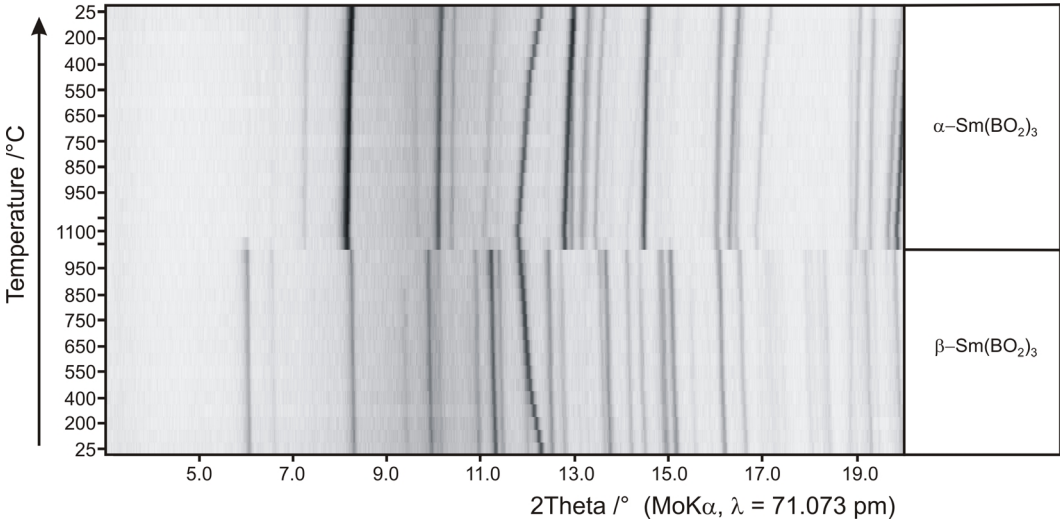


Fig. 4. *In situ* X-ray powder diffraction experiments on  $\beta$ - $\text{Sm}(\text{BO}_2)_3$  at different temperatures.

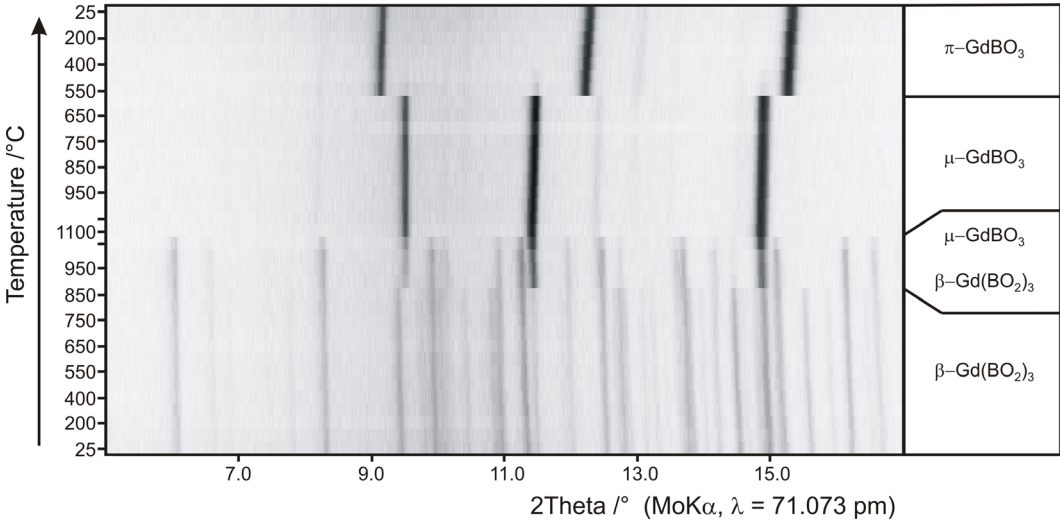


Fig. 5. *In situ* X-ray powder diffraction experiments on  $\beta$ - $\text{Gd}(\text{BO}_2)_3$  at different temperatures.

100 °C steps. After each heating step, diffraction patterns of  $\beta$ - $\text{Sm}(\text{BO}_2)_3$  and  $\beta$ - $\text{Gd}(\text{BO}_2)_3$  were recorded over the angular range  $3^\circ \leq 2\theta \leq 20^\circ$  and  $5^\circ \leq 2\theta \leq 17^\circ$ , respectively. Fig. 4 [ $\beta$ - $\text{Sm}(\text{BO}_2)_3$ ] and Fig. 5 [ $\beta$ - $\text{Gd}(\text{BO}_2)_3$ ] illustrate the temperature programmed X-ray powder diffraction patterns of both compounds.

Interestingly, the thermal behaviour of  $\beta$ -Sm(BO<sub>2</sub>)<sub>3</sub> and  $\beta$ -Gd(BO<sub>2</sub>)<sub>3</sub> is different. For  $\beta$ -Sm(BO<sub>2</sub>)<sub>3</sub>, we observe a transformation of the high-pressure  $\beta$ -phase into the normal-pressure  $\alpha$ -phase in the temperature range 1000–1050 °C. At r. t.,  $\alpha$ -Sm(BO<sub>2</sub>)<sub>3</sub> is the only detectable phase. In contrast,  $\beta$ -Gd(BO<sub>2</sub>)<sub>3</sub> starts to decompose at 900 °C into the high-temperature *orthoborate*  $\mu$ -GdBO<sub>3</sub> [22, 23] and presumably B<sub>2</sub>O<sub>3</sub>. The latter is not detectable in this measurement, because it is liquid at this temperature (melting point of B<sub>2</sub>O<sub>3</sub>: 475 °C). The decomposition process is complete at 1100 °C. Successive cooling to r. t. reveals the transformation of the high-temperature phase  $\mu$ -GdBO<sub>3</sub> into the room-temperature phase  $\pi$ -GdBO<sub>3</sub> in the temper-

ature range 600–500 °C. At r. t., boron oxide remains in an amorphous state.

#### Acknowledgements

The authors gratefully acknowledge the continuous support of this work by Prof. Dr. W. Schnick, Department Chemie and Biochemie of the University of Munich (LMU). Special thanks go to Dr. O. Oeckler, Dr. P. Mayer, and T. Müller for collecting the single crystal data. This work was financially supported by the Deutsche Forschungsgemeinschaft HU 966/2-2 and the European Science Foundation through the COST D30/003/03 network “Development of Materials Chemistry using High Pressures”. H. Huppertz is indebted to the Fonds der Chemischen Industrie for financial support.

- 
- [1] J.-S. Ysker, W. Hoffmann, *Naturwissenschaften* **1970**, 57, 129.
  - [2] G. K. Abdullaev, K. S. Mamedov, G. G. Dzhfarov, *Sov. Phys. Crystallogr.* **1981**, 26, 473.
  - [3] F. Goubin, Y. Montardi, P. Deniard, X. Rocquefelte, R. Brec, S. Jobic, *J. Solid State Chem.* **2004**, 177, 89.
  - [4] C. Sieke, T. Nikelski, Th. Schleid, *Z. Anorg. Allg. Chem.* **2002**, 628, 819.
  - [5] V. I. Pakhomov, G. B. Sil'nitskaya, A. V. Medvedev, B. F. Dzhurinskii, *Inorg. Mater.* **1972**, 8, 1107.
  - [6] H. Müller-Bunz, T. Nikelski, Th. Schleid, *Z. Naturforsch.* **2003**, 58b, 375.
  - [7] G. K. Abdullaev, K. S. Mamedov, G. G. Dzhfarov, *Sov. Phys. Crystallogr.* **1975**, 20, 161.
  - [8] J. Weidelt, *Z. Anorg. Allg. Chem.* **1970**, 374, 26.
  - [9] A. Goriounova, P. Held, P. Becker, L. Bohatý, *Acta Crystallogr. Sect. E: Struct. Rep. Online* **2003**, 59, i83.
  - [10] T. Nikelski, Th. Schleid, *Z. Anorg. Allg. Chem.* **2003**, 629, 1017.
  - [11] H. Emme, T. Nikelski, Th. Schleid, R. Pöttgen, M. H. Möller, H. Huppertz, *Z. Naturforsch.* **2004**, 59b, 202.
  - [12] H. Emme, C. Despotopoulou, H. Huppertz, *Z. Anorg. Allg. Chem.* **2004**, 630, 2450.
  - [13] G. Heymann, H. Huppertz, *J. Solid State Chem.* **2006**, 179, 370.
  - [14] A. Haberer, G. Heymann, H. Huppertz, **2007**, *Z. Naturforsch.* **2007**, 62b, 759.
  - [15] H. Huppertz, *Z. Kristallogr.* **2004**, 219, 330.
  - [16] D. Walker, M. A. Carpenter, C. M. Hitch, *Am. Mineral.* **1990**, 75, 1020.
  - [17] D. Walker, *Am. Mineral.* **1991**, 76, 1092.
  - [18] D. C. Rubie, *Phase Transitions* **1999**, 68, 431.
  - [19] W. Herrendorf, H. Bärnighausen, HABITUS, Universities of Karlsruhe and Giessen, Germany, **1993/1997**.
  - [20] G. M. Sheldrick, SHELXL-97, Program for the Refinement of Crystal Structures, University of Göttingen, Göttingen (Germany) **1997**.
  - [21] G. Demazeau, H. Huppertz, J. Alonso, E. Moran, J. P. Attfield, *Z. Naturforsch.* **2006**, 61b, 1457.
  - [22] E. M. Levin, R. S. Roth, J. B. Martin, *Am. Mineral.* **1961**, 46, 1030.
  - [23] M. Ren, J. H. Lin, Y. Dong, L. Q. Yang, M. Z. Su, L. P. You, *Chem. Mater.* **1999**, 11, 1576.